Polyhedron 30 (2011) 1330–1338

Contents lists available at ScienceDirect

Polyhedron

journal homepage: www.elsevier.com/locate/poly

Synthesis, structural characterization, and properties of heavier alkaline earth complexes containing bis(pyrazolyl)borate or bis(3,5-diisopropylpyrazolyl)borate ligands

Mark J. Saly, Mary Jane Heeg, Charles H. Winter *

Department of Chemistry, Wayne State University, Detroit, MI 48202, United States

ARTICLE INFO

Article history:
Received 29 January 2011
Accepted 15 February 2011
Available online 26 February 2011

Keywords:
Group 2 elements
Calcium
Strontium
Barium
Potassium
Bis(pyrazolyl)borate ligands

ABSTRACT

Treatment of a solid mixture of KBH_4 with six equivalents of 3,5-diisopropylpyrazole ($i\mathrm{Pr_2pzH}$) at 180 °C afforded $\mathrm{KTp}^{i\mathrm{Pr2}}(i\mathrm{Pr_2PzH})_3$ in 53% yield. $\mathrm{KBp}^{i\mathrm{Pr2}}$ was synthesized in 56% yield by treatment of a 1:2 M ratio of KBH_4 and $i\mathrm{Pr_2PzH}$ in refluxing dimethylacetamide. Treatment of MI_2 (M = Ca, Sr, Ba) with two equivalents of KBp or $\mathrm{KBp}^{i\mathrm{Pr2}}$ in tetrahydrofuran afforded $\mathrm{MBp_2(THF)_2}$ (M = Ca, 64%, M = Sr, 81%), $\mathrm{BaBp_2(THF)_4}$ (32%), and $\mathrm{M(Bp}^{i\mathrm{Pr2}})_2\mathrm{(THF)_2}$ (M = Ca, 63%; M = Sr, 61%, M = Ba, 48%) as colorless crystalline solids upon workup. These complexes were characterized by spectral and analytical techniques and by X-ray crystal structure determinations of all complexes except $\mathrm{KBp}^{i\mathrm{Pr2}}$. $\mathrm{KTp}^{i\mathrm{Pr2}}(i\mathrm{Pr_2PzH})_3$ contains one κ^3-N,N,N-$\mathrm{Tp}^{i\mathrm{Pr2}}$ ligand and three κ^1-$i\mathrm{Pr_2pzH}$ ligands, with overall distorted octahedral geometry about the K ion. The $i\mathrm{Pr_2PzH}$ nitrogen–hydrogen bonds are engaged in intramolecular hydrogen bonding to the 2-nitrogen atoms of the $\mathrm{Tp}^{i\mathrm{Pr2}}$ ligand. The solid state structures of $\mathrm{MBp_2(THF)_2}$, $\mathrm{BaBp_2(THF)_4}$, and $\mathrm{M(Bp}^{i\mathrm{Pr2}})_2\mathrm{(THF)_2}$ contain κ^3-N,N,H Bp and $\mathrm{Bp}^{i\mathrm{Pr2}}$ ligands, which form through metal–nitrogen bond formation to the 2-nitrogen atoms of the pyrazolyl fragments and metal–hydrogen bond formation to one boron-bound hydrogen atom per Bp ligand. $\mathrm{SrBp_2(THF)_2}$has the shortest metal–hydrogen interactions among the series. A combination of preparative sublimations, solid state decomposition temperatures, and thermogravimetric analysis demonstrated that $\mathrm{MBp_2(THF)_2}$, $\mathrm{BaBp_2(THF)_4}$, and $\mathrm{M(Bp}^{i\mathrm{Pr2}})_2\mathrm{(THF)_2}$ undergo solid state decomposition at moderate temperatures.

1. Introduction

We recently reported the synthesis, structure, and thermal stability of a series of calcium, strontium, and barium complexes containing tris(pyrazolyl)borate (Tp) ligands and 3,5-dialkyl-substituted analogs [1], and also described the use of $\mathrm{BaTp}_2^{\mathrm{Et2}}$ ($\mathrm{Tp}^{\mathrm{Et2}}$ = tris(3,5-diethylpyrazolyl)borate) and $\mathrm{CaTp_2}$ as precursors for the atomic layer deposition (ALD) growth of BaB_2O_4 and CaB_2O_4 films, respectively, with water as the oxygen source [2]. Significant findings from these reports included documentation of the very high thermal stabilities of the complexes (decomposition temperatures >400 °C for optimized calcium and strontium complexes, ~380 °C for optimized barium complexes), the first reports of metal borate film growth by ALD, and demonstration that the 2:1 boron to metal stoichiometries in $\mathrm{BaTp}_2^{\mathrm{Et2}}$ and $\mathrm{CaTp_2}$ are maintained in the MB_2O_4 films. A drawback of $\mathrm{BaTp}_2^{\mathrm{Et2}}$, $\mathrm{CaTp_2}$, and other group 2 precursors containing Tp-based ligands is their low vapor pressures; temperatures of $\geqslant$200 °C at 0.05 Torr are required to effect sublimation and vapor transport in an ALD reactor [1,2]. ALD precursors must be thermally stable at the film growth temperature, to avoid loss of the self-limited growth mechanism through precursor decomposition [3]. To reduce molecular weight, increase volatility, and hopefully retain high thermal stability observed in the Tp-based precursors, we sought to explore the synthesis and thermal stabilities of group 2 complexes containing bis(pyrazolyl)borate (Bp) ligands and 3,5-disubstituted analogs ($\mathrm{Bp}^{\mathrm{R2}}$). There have been few reports of group 2 complexes that contain Bp-based ligands. Examples include $\mathrm{MBp}_2^{\mathrm{Me2}}\mathrm{(THF)}$ ($\mathrm{Bp}^{\mathrm{Me2}}$ = bis(3,5-dimethylpyrazolyl)borate, M = Ca, Sr, Ba), $\mathrm{MBp}_2^{t\mathrm{Bu}}\mathrm{(THF)}$ ($\mathrm{Bp}^{t\mathrm{Bu}}$ = bis(3-*tert*-butylpyrazolyl)borate, M = Ca, Sr, Ba), and $\mathrm{BaTp}^{\mathrm{Me2}}\mathrm{Bp}^{\mathrm{Me2}}$ ($\mathrm{Tp}^{\mathrm{Me2}}$ = tris(3,5-dimethylpyrazoly)borate) [4]. Sohrin carried out ion extraction studies of the group 2 ions using Bp ligands, and found that significant extraction did not occur for Ca^{2+}, Sr^{2+}, or Ba^{2+} [5]. The solid state structures of $\mathrm{MgBp(THF)(\mu\text{-}Cl)_2MgBp(THF)_2}$, $\mathrm{MgBp_2(THF)}$, and $\mathrm{MgBp_2(THF)_2}$ have been described [6]. We have recently reported the synthesis, structure, and properties of $\mathrm{M(Bp}^{t\mathrm{Bu2}})_2$ (M = Ca, Sr, Ba) and $\mathrm{Ba(Bp}^{t\mathrm{Bu2}})_2\mathrm{(THF)}$

---

* Corresponding author. Tel.: +1 313 577 5224; fax: +1 313 577 8289.
E-mail address: chw@chem.wayne.edu (C.H. Winter).

0277-5387/$ - see front matter © 2011 Elsevier Ltd. All rights reserved.
doi:10.1016/j.poly.2011.02.026

(Bp^{tBu2} = bis(3,5-di-*tert*-butylpyrazolyl)borate, and noted that extreme distortions of the Bp^{tBu2} ligands are present within the coordination spheres due to intraligand and interligand *tert*-butyl steric crowding [7].

Herein, we report the synthesis, structure, and properties of a series of calcium, strontium, and barium complexes containing Bp and Bp^{iPr2} ligands. These complexes also incorporate tetrahydrofuran ligands. In addition, attempted synthesis of the key starting material KBp^{iPr2} by a literature method instead afforded the structurally novel complex $KTp^{iPr2}(iPr_2pzH)_3$ (Tp^{iPr2} = tris(3,5-diisopropylpyrazolyl)borate; iPr_2pzH = 3,5-diisopropylpyrazole). An alternate procedure for the synthesis of KBp^{iPr2} is reported.

2. Results and discussion

2.1. Synthetic aspects

KBp was prepared in 72% yield using a literature procedure, which entailed thermolysis of a 1:2 M ratio mixture of solid KBH_4 and pyrazole at 120 °C [8]. A previously reported synthesis of KBp^{iPr2} (**1**) relied upon heating a solid mixture of KBH_4 and iPr_2PzH in a 1:2 stoichiometry at 120 °C, followed by crystallization from hexane [9]. However, multiple attempts to reproduce this synthesis instead afforded $KTp^{iPr2}(iPr_2PzH)_3$ (**2**). Optimization involved conducting the thermolysis at 180 °C with a 1:6 stoichiometry of KBH_4 and iPr_2PzH, which afforded colorless crystals of **2** in 53% yield (Eq. (1)). For comparison, KTp^{iPr2} was previously synthesized by heating a 1:3 M ratio of solid KBH_4 and iPr_2PzH at 260 °C, followed by crystallization from pentane [10]. In the present work, **1** was synthesized in 56% yield by treatment of a 1:2 M ratio of KBH_4 and iPr_2PzH in refluxing dimethylacetamide (DMAC), as described in Section 4 (Eq. (2)). Complexes **1** and **2** are very soluble in tetrahydrofuran and toluene.

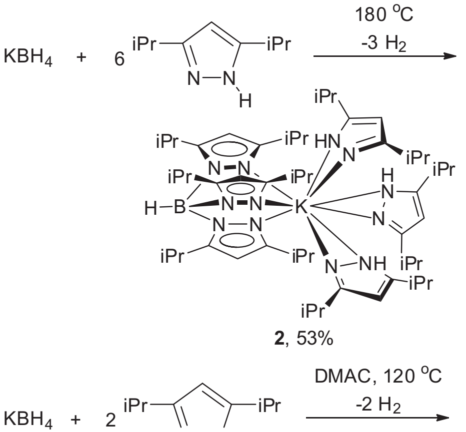

2, 53%

(1)

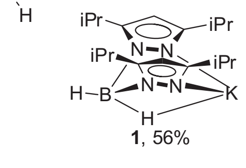

1, 56%

(2)

Treatment of MI_2 (M = Ca, Sr, Ba) with two equivalents of KBp or **1** yielded **3**–**8** as colorless crystalline solids upon workup (Eq. (3)). Complexes **3** and **4** are very soluble in tetrahydrofuran and diethyl ether and are moderately soluble in hexane. By contrast, **5** is insoluble in hexane and diethyl ether, but is soluble in tetrahydrofuran. Complexes **6**–**8** are soluble in hexane, and their solubilities increase in the order **6** < **7** < **8**.

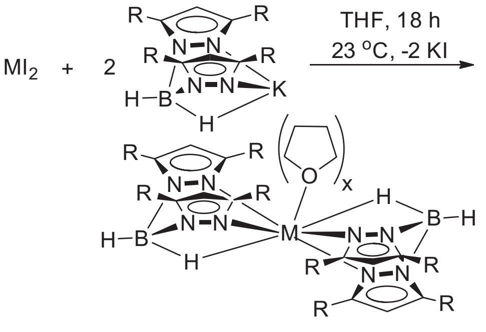

(3)

3, M = Ca, R = H, x = 2, 64%
4, M = Sr, R = H, x = 2, 81%
5, M = Ba, R = H, x = 4, 32%
6, M = Ca, R = iPr, x = 2, 63%
7, M = Sr, R = iPr, x = 2, 61%
8, M = Ba, R = iPr, x = 2, 48%

The compositions of **1**–**8** were assessed by spectral and analytical data, and by X-ray crystal structure determinations for **2–8**. In the ^1H NMR spectra of **1** and **6–8**, the 4-H atoms of the iPr_2pz groups were observed at δ 5.78 and 5.76, respectively. Additional resonances belonging to the magnetically inequivalent isopropyl groups were observed. The ^1H NMR spectra for **6–8** also contained resonances corresponding to two tetrahyrofuran ligands centered at δ 3.61 and 1.79, respectively. Similar to **1** and **6–8**, the ^1H NMR spectra for **2** showed the 4-H atom resonance of the Tp^{iPr2} ligand at δ 5.70, as well as the resonances from the magnetically inequivalent isopropyl groups. The three iPr_2pzH ligands in **2** showed the 4-H atom resonance at δ 5.84 and the methine and methyl resonances of the isopropyl groups at δ 2.60 and 1.21, respectively. A broad N-bound H atom resonance appeared at δ 9.98. Broad B-bound H atom resonances for **1** and **2** were centered at δ 3.45 and 4.90, respectively. The B-bound H atom resonances were not clearly observed in the ^1H NMR spectra of **6**–**8**, because the signals were too broad and overlapped with the downfield isopropyl methine and tetrahydrofuran 2-H atom resonances. The ^1H NMR spectra for **3**–**5** contained three resonances belonging to the three different protons from the pyrazolyl ring of the Bp ligand, with the 4-H atom resonance observed at about δ 6.0. All of the expected C atom resonances were observed in the $^{13}C\{^1H\}$ NMR spectra for **1**–**5**, **7**, and **8**. However, the $^{13}C\{^1H\}$ NMR spectrum for **6** only showed one C atom resonance at 25.79 ppm corresponding to the isopropyl methyl groups, instead of the expected two resonances. The methyl C atom resonances appear to overlap, which is supported by the inequivalent methyl proton resonances observed in the ^1H NMR spectrum of **6**. In the infrared spectra of **1** and **3–8**, the B–H stretches are observed in the range of 2248–2448 cm^{-1}. The C–N stretching frequencies are observed between 1492–1502 cm^{-1} and 1527–1532 cm^{-1} for **3**–**5** and **1** and **6**–**8**, respectively. The shift to higher wavenumbers for the C–N stretches in **1** and **6**–**8** appears to arise from the isopropyl substituents on the pyrazolyl groups, compared to H atoms in **3**–**5**. The infrared spectrum of **2** showed a B–H stretch at 2469 cm^{-1}, which is consistent with one B–H bond. Two C–N stretches in **2** were observed at 1529 and 1565 cm^{-1}, and correspond to the B-bound iPr_2pz moieties and the iPr_2pzH ligands in **2**. Furthermore, two N–H stretches at 3261 and 3358 cm^{-1} were observed, which arise from the iPr_2pzH ligands.

2.2. Structural aspects

The X-ray crystal structures of **2–8** were determined to establish the geometry about the metal centers and the bonding modes of the Bp and Bp^{iPr2} ligands. Experimental crystallographic data are summarized in Table 1, selected bond lengths and angles are given in Tables 2–5, and perspective views are presented in Figs. 1–5. Complexes **7** and **8** are isostructural with **6**, and are not discussed specifically herein, but have been deposited with the Cambridge Crystallographic Structural Database.

A perspective view of **2** is shown in Fig. 1. The complex contains one κ^3-N,N,NTp^{iPr2} ligand and three κ^1-*i*Pr$_2$pzH ligands, with overall distorted octahedral geometry about the K ion. The K–N bond distances associated with the Tp^{iPr2} ligand are 2.795(2), 2.823(2), and 2.913(2) Å, compared to very similar values of 2.782(3), 2.784(3), and 2.832(3) Å for the *i*Pr$_2$pzH ligands. The average K–N bond distance found in **2** (2.82(5) Å) is similar to the related values in KTp^{tBu2} (K–N$_{avg}$ = 2.73(2) Å) [11a], KTp^{Pic,Me}(H$_2$O)$_2$ (Pic = 5-α-picolyl, K–N$_{avg}$ = 2.9(1) Å) [12], KTp^{3Py,Me}(H$_2$O) (3Py = 3-pyridyl, K–N$_{avg}$ = 2.90(8) Å) [12], and KTp^{R,H} (R = 2-methoxy-1,1-dimethylethyl, K–N$_{avg}$ = 2.692(2) Å) [13]. The N-bound H atom of each *i*Pr$_2$pzH ligand is directed toward the 2-N atoms of the Tp^{iPr2} ligand, suggesting the presence of weak intramolecular N–H···N hydrogen bonds. The pyrazolyl 2-N···H distances are 2.48(3) (to N(1)), 2.17(4) (to N(3)), and 2.26(3) Å (to N(5)). The sum of the van der Waals radii for N and H atoms is 2.75 Å [14], so these interactions are consistent with hydrogen bonds. Further evidence of hydrogen bonding comes from broad N–H bond stretches in the infrared spectrum of **2** at 3261 and 3358 cm^{-1}. A sharp band at 3374 cm^{-1} was previously reported to arise from a non-hydrogen bonded N–H stretch in a *i*Pr$_2$pzH adduct [12]. The structure of **2** is similar to that of [PbTp^{Me2}(Me$_2$pzH)$_3$]Cl, which contains one κ^3-Tp^{Me2} ligand and three Me$_2$pzH ligands arrayed in a distorted octahedral geometry [15]. Unlike the hydrogen bonding in **2**, the three N-bound H atoms of the Me$_2$pzH ligands in [PbTp^{Me2}(Me$_2$pzH)$_3$]Cl form hydrogen bonds to the chloride counterion, apparently due to its higher basicity compared to the Tp^{Me2}N atoms that are bonded to the Pb^{2+} ion. In **2**, the 2-N atoms of the Tp^{iPr2} ligand are the most basic within the molecule, and it is not surprising that these N atoms act as hydrogen bond acceptors.

The molecular structures of **3–5** are similar and their perspective views are shown in Figs. 2–4. Complexes **3** and **4** crystallize as monomeric complexes containing two Bp and two tetrahydrofuran ligands, with a coordination number of eight. By contrast, **5** contains two Bp and four tetrahydrofuran ligands, affording a coordination number of ten. In **3–5**, the Bp ligands adopt the κ^3-N,N,H coordination mode, through M–N bond formation to the 2-N atoms of the pyrazolyl fragments and M–H bond formation to one B-bound H atom per Bp ligand. κ^3-N,N,H coordination of Bp ligands is commonly observed in many metal complexes [16]. Complexes **3–5** have M···H–B distances of 2.77(2) and 3.01(3) Å, 2.59(6) and 2.73(4) Å, and 3.23(3) and 3.33(2) Å, respectively. The sum of van der Waals radii for Ca + H, Sr + H, and Ba + H are 3.51, 3.69, and

Table 2
Selected atomic distances (Å) and angles (°) for **2**.

K–N(1)	2.795(2)
K–N(3)	2.823(2)
K–N(5)	2.913(2)
K–N(7)	3.466(3)
K–N(8)	2.780(3)
K–N(9)	2.833(2)
K–N(10)	3.396(2)
K–N(11)	3.453(3)
K–N(12)	2.781(3)
N(1)–H(N7)	2.48(3)
N(3)–H(N10)	2.17(4)
N(5)–H(N11)	2.26(3)
K–N(1)–N(2)	115.89(16)
K–N(3)–N(4)	114.80(15)
K–N(5)–N(6)	111.51(15)
B–N(2)–N(1)	121.1(2)
B–N(4)–N(3)	121.7(2)
B–N(6)–N(5)	121.5(2)
N(2)–B–N(4)	111.0(2)
N(2)–B–N(6)	110.3(2)
N(4)–B–N(6)	109.2(2)

Table 3
Selected atomic distances (Å) and angles (°) for **3** and **4**.

	3	4
M–O(1)	2.381(2)	2.567(4)
M–O(2)	2.394(2)	2.560(4)
M–N(1)	2.451(2)	2.624(5)
M–N(3)	2.491(2)	2.641(5)
M–N(5)	2.443(2)	2.634(5)
M–N(7)	2.477(2)	2.676(5)
M–N(1)–N(2)	114.76(14)	111.7(4)
M–N(3)–N(4)	114.38(15)	110.8(4)
M–N(5)–N(6)	118.64(15)	109.6(4)
M–N(7)–N(8)	117.47(15)	108.7(4)
B(1)–N(2)–N(1)	119.26(19)	120.2(5)
B(1)–N(4)–N(3)	118.82(19)	120.2(5)
B(2)–N(6)–N(5)	119.3(2)	119.8(5)
B(2)–N(8)–N(7)	119.4(2)	120.1(6)
N(2)–B(1)–N(4)	109.2(2)	108.9(5)
N(6)–B(2)–N(8)	109.2(2)	109.4(6)
O(1)–M–O(2)	79.34(6)	81.51(14)

Table 1
Crystal data and data collection parameters for **2–6**.

	2	3	4	5	6	7	8
Formula	$C_{54}H_{94}BKN_{12}$	$C_{20}H_{32}B_2CaN_8O_2$	$C_{20}H_{32}B_2N_8O_2Sr$	$C_{28}H_{48}B_2BaN_8O_4$	$C_{44}H_{80}B_2CaN_8O_2$	$C_{44}H_{80}B_2N_8O_2Sr$	$C_{44}H_{80}BaB_2N_8O_2$
Formula weight	961.32	478.24	525.78	719.70	814.86	862.40	912.12
Space group	$P\bar{1}$	$P2_1/c$	$P2_1/n$	$P2_1/c$	$P2/c$	$P2/c$	$P2/c$
a (Å)	13.4823(4)	8.1820(3)	11.5239(11)	10.0475(3)	9.0091(6)	9.0253(4)	8.9791(5)
b (Å)	14.4362(4)	32.1359(13)	14.3932(14)	18.4400(5)	12.5037(7)	12.5252(6)	12.5148(7)
c (Å)	15.0315(4)	9.6550(4)	16.1877(17)	18.6347(5)	22.2896(14)	22.6409(10)	22.8178(13)
α	89.916(2)						
β	88.740(2)	97.639(2)	108.581(7)	99.0340(10)	99.030(4)	99.414(3)	97.585(3)
γ	88.405(2)						
V (Å^3)	2923.79(14)	2516.42(17)	2545.0(4)	3409.73(17)	2479.7(3)	2524.9(2)	2541.6(2)
Z	2	4	4	4	2	2	2
T (K)	100(2)	100(2)	100(2)	100(2)	100(2)	100(2)	100(2)
λ (Å)	0.71073	0.71073	0.71073	0.71073	0.71073	0.71073	0.71073
ρ_{calc} (g cm^{-3})	1.092	1.262	1.372	1.402	1.091	1.134	1.192
μ (mm^{-1})	0.135	0.282	2.151	1.209	0.168	1.108	0.822
R (F) (%)	9.02	5.89	9.02	2.85	6.64	6.94	4.83
Rw (F) (%)	20.36	13.22	14.86	6.85	12.22	13.15	11.55

$R(F) = \Sigma||F_o| - |F_c||/\Sigma|F_o|$; $Rw(F) = [\Sigma w(F_o{}^2 - F_c{}^2)^2/\Sigma w(F_o{}^2)^2]^{1/2}$ for $I > 2\sigma(I)$.

Table 4
Selected atomic distances (Å) and angles (°) for **5**.

Ba–O(1)	2.791(1)
Ba–O(2)	2.788(1)
Ba–O(3)	2.824(1)
Ba–O(4)	2.919(1)
Ba–N(1)	2.902(2)
Ba–N(3)	2.852(2)
Ba–N(5)	2.886(2)
Ba–N(7)	2.862(2)
Ba–N(1)–N(2)	118.34(1)
Ba–N(3)–N(4)	120.82(1)
Ba–N(5)–N(6)	115.86(1)
Ba–N(7)–N(8)	115.64(1)
B(1)–N(2)–N(1)	121.16(2)
B(1)–N(4)–N(3)	120.66(2)
B(2)–N(6)–N(5)	121.77(2)
B(2)–N(8)–N(7)	121.45(2)
N(2)–B(1)–N(4)	109.91(2)
N(6)–B(2)–N(8)	110.68(2)
O(1)–Ba–O(2)	139.28(4)
O(1)–Ba–O(3)	142.61(4)
O(1)–Ba–O(4)	72.77(4)
O(2)–Ba–O(3)	72.94(4)
O(2)–Ba–O(4)	147.42(4)
O(3)–Ba–O(4)	80.34(4)

Table 5
Selected atomic distances (Å) and angles (°) for **6**.

Ca–O(1)	2.431(2)
Ca–N(1)	2.478(2)
Ca–N(3)	2.562(2)
Ca–N(1)–N(2)	118.22(13)
Ca–N(3)–N(4)	110.48(12)
B–N(2)–N(1)	117.55(18)
B–N(4)–N(3)	119.25(17)
N(2)–B–N(4)	110.9(2)
O(1)–Ca–O(1)′	149.28(8)

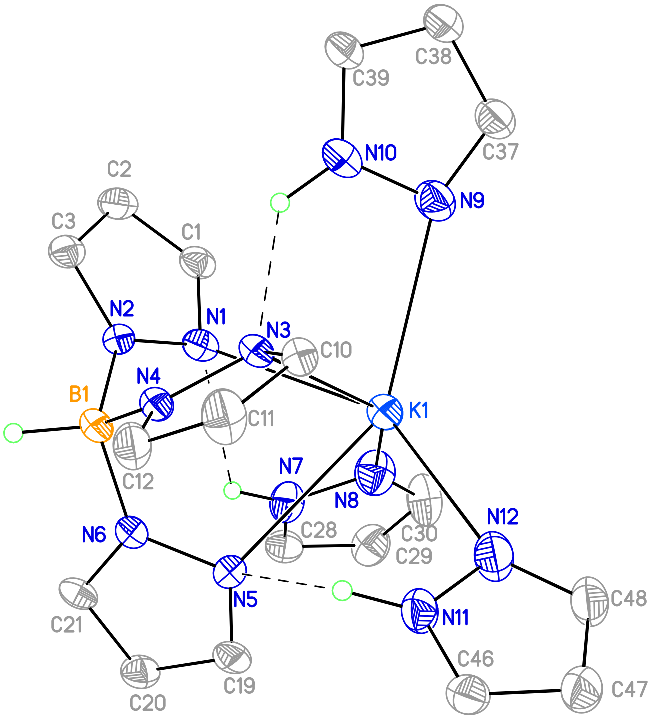

Fig. 1. Perspective view of **2** with thermal ellipsoids at the 50% probability level. The isopropyl groups have been removed for clarity.

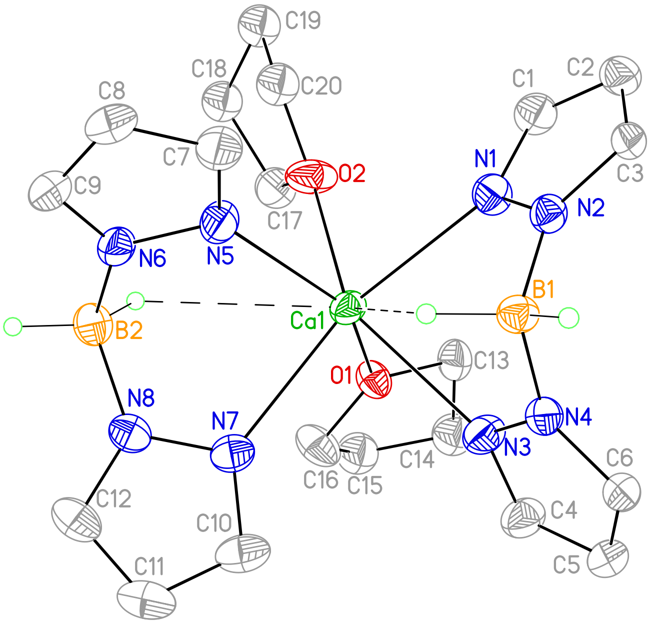

Fig. 2. Perspective view of **3** with thermal ellipsoids at the 50% probability level.

3.88 Å, respectively [14]. As such, strong M–H interactions are present in **3**–**5**. The average Ca–N bond distance in **3** is 2.47(2) Å, which is similar to those in CaTp$_2$ (avg = 2.44(2) Å) [4], CaTp$_2^{\mathrm{Me2}}$ (avg = 2.454(2) Å) [4], and CaTp$_2^{\mathrm{Et2}}$ (avg = 2.459(6) Å) [1]. The average Sr–N distance in **4** (2.64(2) Å) is slightly longer than those in SrTp$_2$ (avg = 2.593(19) Å) and SrTp$_2^{\mathrm{Et2}}$ (avg = 2.606(9) Å) [1]. The average Ba–N distance in **5** is 2.88(2) Å, which again is longer than those in Tp-based complexes such as BaTp$_2^{\mathrm{Me2}}$ (avg = 2.754(3) Å, 2.760(1) Å) [4,17] and BaTp$_2^{\mathrm{Et2}}$ (avg = 2.78(2) Å) [1]. The slightly longer M–N distances in **3**–**5**, compared to related Tp complexes, is likely related to the higher coordination numbers in the former, which arise through tetrahydrofuran coordination and M–H bond formation. The M–O distances in **3** and **4** are 2.387(7) and 2.564(4) Å, respectively. The Ba–O bond lengths in **5** range from 2.788(1) to 2.919(1) Å, with an average of 2.83(6) Å. The average N–B–N bond angles in **3**–**5** are 109.2(2)°, 109.2(3)°, and 110.3(4)°, respectively, indicating tetrahedral geometry about the boron atoms.

A perspective view of **6** is shown in Fig. 5. Complex **6** is eight coordinate, and contains two κ^3-N,N,H-Bp$^{i\mathrm{Pr2}}$ and two tetrahydrofuran ligands. The Ca–H distance in **6** (2.95(2) Å) is similar to the values in **3** (2.77(2), 3.01(3) Å), but is considerably longer than the related distances in CaTp$_2^{t\mathrm{Bu}}$ (2.47(2) Å) [18] and Ca(C$_5$H$_2$(SiMe$_3$)$_3$)(HBEt$_3$)(THF)$_2$ (2.21(4) Å) [19]. The Ca–H interactions in **3**, **6**, and previously reported borohydride complexes are electrostatic, and the Ca–H distances appear to be determined by steric interactions about the Ca ion. In **3** and **6**, the coordination spheres are crowded with tetrahydrofuran ligands, which do not permit enough space for shorter Ca–H bonds. The Ca–N distances in **6** are 2.478(2) and 2.562(2) Å, respectively, with a Ca–O distance of 2.431(2) Å and a N–B–N bond angle of 110.9(2)°. The longer Ca–N distances in **6** versus **3** are likely related to the larger steric profile of the Bp$^{i\mathrm{Pr2}}$ ligand compared to the Bp ligand. The B–N–N–Ca torsion angles in **6** are 4.4(2) (B–N(2)–N(1)–Ca) and 31.8(2)° (B–N(4)–N(3)–Ca), which are larger than those of **3** due to the higher steric congestion about the Ca ion arising from the isopropyl groups in **6**.

In **3** and **5**, the two M–H interactions are *anti* with respect to each other within each molecule, whereas **4** contains *syn* Sr–H units within each molecule. Such an arrangement in **4** also requires

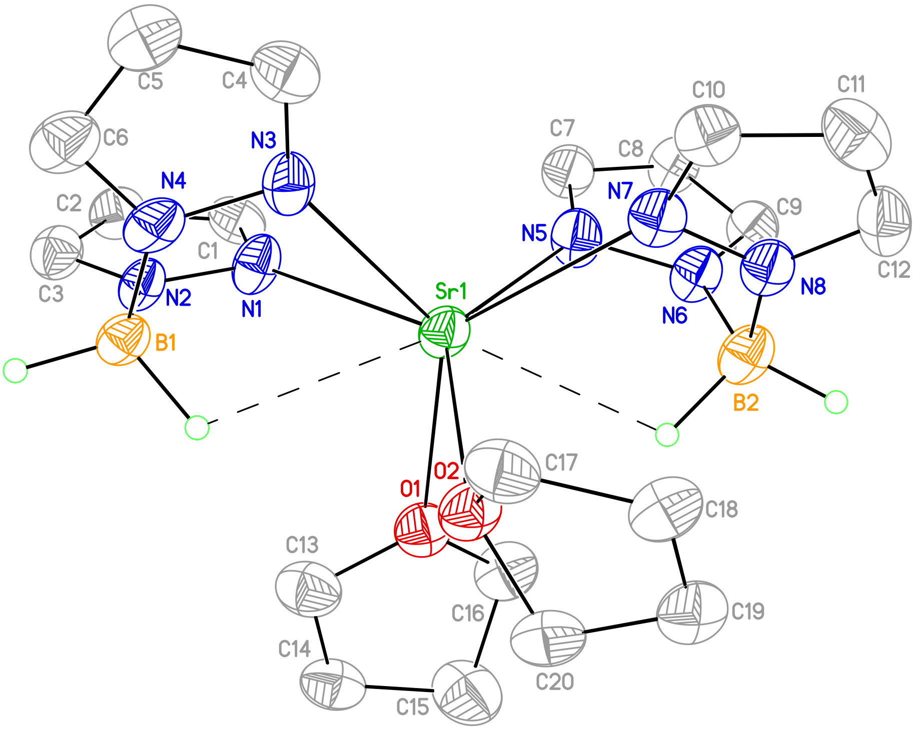

Fig. 3. Perspective view of **4** with thermal ellipsoids at the 50% probability level.

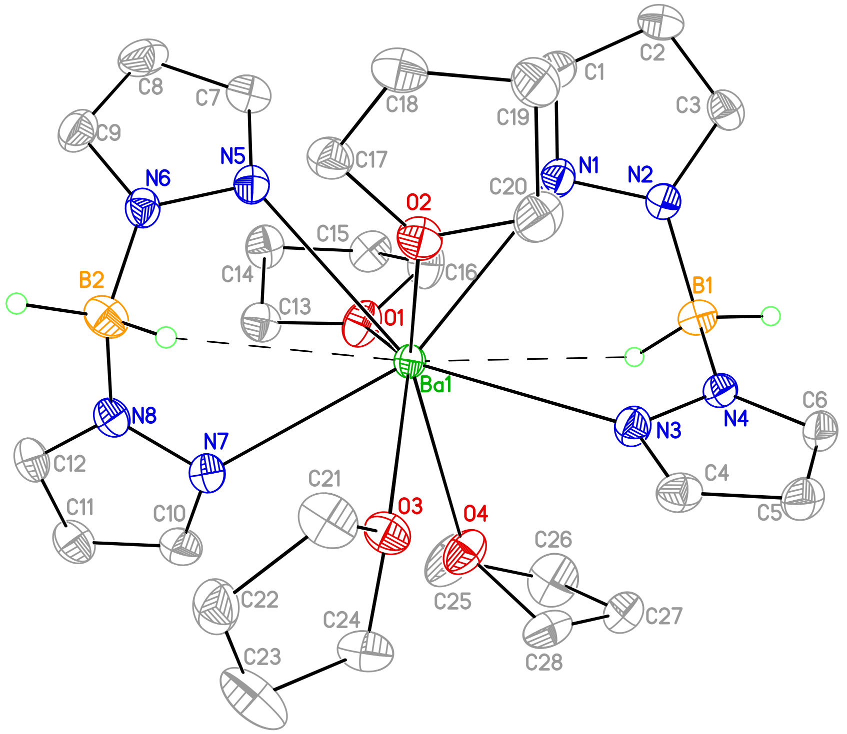

Fig. 4. Perspective view of **5** with thermal ellipsoids at the 50% probability level.

cis-coordination of the tetrahydrofuran ligands. A Cambridge Crystallographic Database search of compounds containing Bp-based ligands revealed no previous examples of *syn* M–H units such as those found in **4**. The most common orientation for Bp-based ligands is with the M···H–B and pyrazolyl moieties *anti* to each other [6,20–23]. Divalent transition metal Bp complexes of the formula MBp_2 contain κ^3-N,N,H Bp ligands where the coordinated H atoms are 90° from one another in the equatorial plane [24,25]. Complexes **3**, **5**–**8**, $MgBp_2(THF)$ [6], MBp_2^{tBu2} (M = Sr, Ba) [7], $MBp_2^{tBu2}(THF)$ [7], $Y(Bp)_3$ [21], and $U(Bp^{Me2})_3$ [22] all contain *anti* Bp and Bp^{Me2} ligand conformations within the metal coordination spheres, further illustrating the structural novelty of **4**.

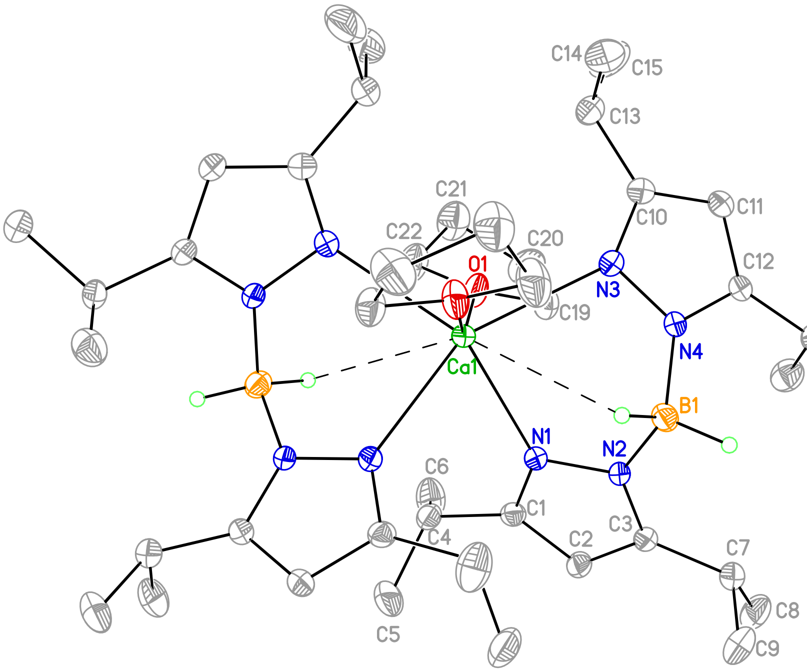

Fig. 5. Perspective view of **6** with thermal ellipsoids at the 50% probability level.

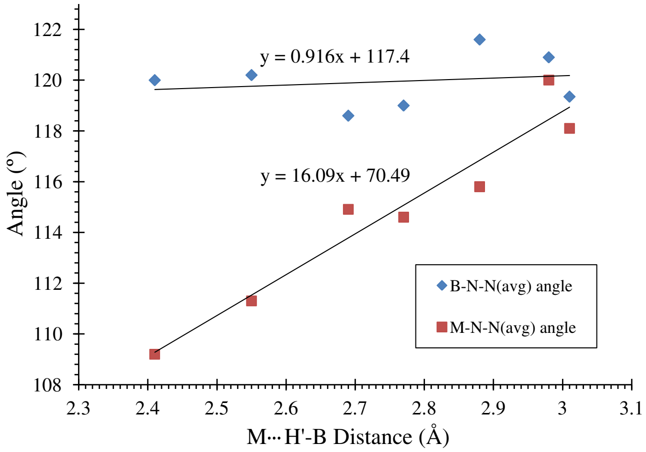

Fig. 6. Plot of M···H′–B distances (Å) versus average B–N–N and M–N–N angles (°).

Table 6 contains structural data for **3**–**5**, MgBp$_2$(THF) [6], MBp$_2^{tBu2}$ (M = Sr, Ba) [7], and BaBp$_2^{tBu2}$(THF) [7] associated with the M···H–B interactions. To allow direct comparison of the M···H–B interactions, the M–H bond lengths were normalized to the ionic size of Ca^{2+} by subtracting or adding the difference between the M^{2+} and Ca^{2+} ionic radii to the M···H–B distance of the other group 2 ions. The data reveal that the Sr···H–B interactions in **4** are the shortest among **3**–**5**, with Sr···H′–B distances of 2.59(6) and 2.73(4) Å. Stabilization of the *syn* conformation of **4** is probably a result of the ionic size, tetrahydrofuran ligand arrangement, and formation of stronger Sr···H–B interactions offsetting the slight increase in energy upon eclipsing the pyrazolyl moieties. The six membered B–(NN)$_2$–M chelate rings in **3**–**8** form boat conformations, due to the M–H bond formation. Depending on the strength of the M···H–B interaction, the boat can be shallow or deep. A plot of the M···H′–B distances versus the average B–N–N and M–N–N angles is shown in Fig. 6. The plot indicates that the B–N–N angles vary little as a function of the M···H′–B distances, whereas the M–N–N bond angles change significantly with respect to the M···H′–B distance. Hence, the M–N bonds act as hinges for the M–H interactions, and thus the extent of the M–H interactions and depth of the boat are directly related to the M–N–N angles. Such flexibility of the M–N–N angles is facilitated by the nondirectional, ionic M–N bonds.

The present study allows us to compare the structural distortions of the Bp and Bp^{iPr2} ligands in **3**–**6** with those that occur in MBp$_2^{tBu2}$ (M = Sr, Ba) and BaBp$_2^{tBu2}$(THF) [7]. In our previous paper describing Sr and Ba complexes containing Bp^{tBu2} ligands [7], the B–N–N–M torsion angles ranged from 20.0° to 60.9°, which are larger than the corresponding values found in MgBp$_2$(THF) [6], Y(Bp)$_3$ [21], and U(Bp^{Me2})$_3$ [22]. The B–N–N–M torsion angles in **3** (0.72–8.62°) and **4** (2.39–7.37°) imply low steric congestion about the metal ions. The corresponding values in **5** are larger (0.20–20.02°) and suggest more steric congestion, consistent with the higher coordination number in **5** compared to **3** and **4**. The B–N–N–Ca torsion angles in **6** are 4.4(2) (B–N(2)–N(1)–Ca) and 31.8(2)° (B–N(4)–N(3)–Ca), which are larger than those of **3**–**5** due to the higher steric congestion about the Ca ion arising from

Table 6
Selected metrical data for **3**–**5** and MgBp$_2$(THF).

Complex	M···H–B (Å)	M···H′–B[a] (Å)	B–N–N$_{avg}$ (°)	M–N–N$_{avg}$ (°)
MgBp$_2$(THF) [6]	2.69	2.97	118.6	114.91
Sr(Bp^{tBu2})$_2$ [7]	2.56(1)	2.39(1)	115.80(7)	
	2.59(1)	2.41(1)		
Ba(Bp^{tBu2})$_2$ [7]	2.66(2)	2.31(2)	116.28(12)	
	2.71(2)	2.36(2)		
Ba(Bp^{tBu2})$_2$(THF) [7]	2.83(2)	2.48(2)	115.9(2)	
	2.89(2)	2.54(2)		
3	2.77(2)	2.77(2)	119.0(2)	114.6(2)
	3.01(3)	3.01(3)	119.35(5)	118.1(6)
4	2.73(4)	2.55(4)	120.2(0)	111.3(5)
	2.59(6)	2.41(6)	120.0(2)	109.2(5)
5	3.33(2)	2.98(2)	120.9(3)	120(1)
	3.23(3)	2.88(3)	121.6(2)	115.8(1)

[a] Values are normalized to the ionic size of Ca^{2+} by subtracting or adding the difference between the M^{2+} and Ca^{2+} ionic radii to the M···H–B distance.

the isopropyl groups in **6**. The B–N–N–M torsion angles found in **3**–**6** (0.2–31.8°) are in the same range as those found in TlBp^{tBu2} (20.8, 23.7°) [11b], and U(Bp^{Me2})$_3$ (17.6–21.3°) [23], and are much smaller than the values found in MBp$_2^{tBu2}$ (M = Sr, Ba) and BaBp$_2^{tBu2}$(THF) [7]. Accordingly, the increased steric congestion upon coordination of tetrahydrofuran in **3**–**6** does not lead to large distortions of the Bp or Bp^{iPr2} ligand bonding to the metal ions. B–N–N–M torsion angles have been proposed as a measure of the sterically-induced twisting of the pyrazoyl moieties in Tp-based ligands [7,11]. The B–N–N–K torsion angles in **2** range from 40.7(3)° to 44.4(3)° (avg = 42(2)°), which are nearly double the corresponding torsion angles found in KTp^{tBu2}(C$_6$H$_6$) (avg = 23.4°), TlBp^{tBu2} (avg = 22.8°), and CsTp^{tBu2} (avg = 24.4°) [11a]. The larger torsion angles in **2**, compared to complexes containing the Tp^{tBu2} ligand, are caused by the extreme steric crowding that arises upon coordinating one Tp^{iPr2} and three *i*Pr$_2$pzH ligands to the K ion.

2.3. Evaluation of thermal stability and volatility

Complexes **3**–**8** were studied by preparative sublimations and solid state decomposition temperature determinations to assess their volatilities and thermal stabilities. Preparative sublimations of **3**–**8** between 160 and 220 °C at 0.05 Torr led to the vapor transport of complex mixtures of compounds, among which pyrazole (from **3** to **5**) or 3,5-diisopropylpyrazole (from **6** to **8**) were identified by ^{1}H NMR spectroscopy. The yields of sublimed materials were low, suggesting extensive decomposition prior to sublimation upon heating in the sublimation tube. The melting points for **3**, **4**, and **6**–**8** are 116, 121, 113, 168, and 167 °C, respectively. Upon melting, the liquid compounds exhibited gas evolution, which most likely corresponds to loss of the tetrahydrofuran ligands. After melting, **3**, **4**, and **6–8** remained colorless liquids until reaching temperatures between 330 and 360 °C, over which range the clear melts underwent rapid darkening (**3**, 360 °C; **4**, 330 °C; **6**, 340 °C; **7**, 350 °C; **8**, 348 °C). Complex **5** melts at a higher temperature than the others (281 °C), and likewise shows gas evolution upon reaching the liquid state. The clear, colorless melt of **5** turned black rapidly at 330 °C, indicating thermal decomposition.

3. Conclusions

We have prepared the novel potassium complex **2** upon treatment of KBH$_4$ with six equivalents of *i*Pr$_2$pzH. The solid state structure of **2** exhibits large distortions of the Tp^{iPr2} ligand due to accommodation of the sterically demanding isopropyl groups within the coordination sphere. An improved synthesis of **1** was also developed. Treatment of KBp or **1** with MI$_2$ (M = Ca, Sr, Ba) in tetrahydrofuran afforded **3**–**8**. The crystal structures of **3**–**8** showed κ^3-N,N,H-coordination of the Bp and Bp^{iPr2} ligands as well as coordination of two (**2**–**4**, **6**–**8**) or four (**5**) tetrahydrofuran ligands. Examination of the B–N–N–M torsion angles demonstrated that distortions of the Bp and Bp^{iPr2} ligand bonding to the metal ions are smaller than those observed in the previously reported complexes MBp$_2^{tBu2}$ (M = Sr, Ba) and BaBp$_2^{tBu2}$(THF) [7], thus indicating that tetrahydrofuran coordination does not drastically increase the steric crowding in the coordination spheres of these complexes. Complexes **3**–**6** decompose in the solid state upon heating to afford complex mixtures of products, and are not volatile.

4. Experimental

4.1. General considerations

All reactions were performed under argon using either standard glovebox or Schlenk line techniques. Tetrahydrofuran was distilled from sodium benzophenone ketyl. Hexane was distilled from P$_2$O$_5$. KBp [8]^7 and *i*Pr$_2$pzH [10] were synthesized according to literature procedures. All other starting materials were purchased from Acros or Aldrich Chemical Company and were used as received.

^{1}H and ^{13}C{^{1}H} NMR spectra were obtained at 400, 300, 125, or 75 MHz in methylene chloride-*d*$_2$, benzene-*d*$_6$, or acetone-*d*$_6$. Infrared spectra were obtained using Nujol as the medium. Elemental analyses were performed by Midwest Microlab, Indianapolis, Indiana. Melting points were obtained on an Electrothermal Model 9200 melting point apparatus and are uncorrected. TGA was conducted on a Perkin–Elmer Pyris 1 TGA system between 50 and 550 °C, using nitrogen as the flow gas with a heating rate of 10 °C/min.

*4.2. Preparation of KBp^{iPr2} (**1**)*

A 100-mL round-bottomed flask was charged with KBH$_4$ (0.794 g, 14.72 mmol), *i*Pr$_2$pzH (5.000 g, 32.42 mmol), anhydrous DMAC (50 mL), and a stir bar. The mixture was slowly heated in an oil bath to 120 °C, while carefully monitoring hydrogen evolution. Once gas evolution ceased (~670 mL), the oil bath was removed and the reaction mixture was allowed to cool to ambient temperature. The DMAC was then removed under reduced pressure. The resulting crude mixture was then heated to ~130 °C and the excess *i*Pr$_2$pzH was distilled at 0.05 Torr. The product was washed with cold hexane (30 mL) and was isolated by vacuum filtration. To remove any unreacted KBH$_4$, the solid was further dissolved in methylene chloride (25 mL) and the solution was filtered through a medium glass filter frit. The methylene chloride was removed under reduced pressure to afford **1** as a white powder (2.913 g, 56%). The analytical sample was obtained by crystallization of 0.250 g of **1** from toluene (20 mL) at −23 °C: mp 168–169 °C; IR (Nujol, cm^{-1}) ν_{B-H} = 2248–2438, ν_{C-N} = 1526; ^{1}H NMR (CD$_2$Cl$_2$, 23 °C, δ) 5.78 (s, 2H, 4-C*H*), 3.45 (broad s, 2H, B*H*$_2$,), 3.21 (septet, *J* = 6.8 Hz, 2H, C*H*(CH$_3$)$_2$), 2.80 (septet, *J* = 6.8 Hz, 2H, C*H*(CH$_3$)$_2$), 1.11 (d, *J* = 6.6 Hz, 12H, CH(C*H*$_3$)$_2$), 1.07 (d, *J* = 6.9 Hz, 12H, CH(C*H*$_3$)$_2$); ^{13}C{^{1}H} NMR (CD$_2$Cl$_2$, 23 °C, ppm) 158.95 (s, *C*$_q$), 155.97 (s, *C*$_q$), 96.96 (s, 4-*C*H), 28.32 (s, *C*H(CH$_3$)$_2$), 26.42 (s, *C*H(CH$_3$)$_2$), 23.61 (s, CH(*C*H$_3$)$_2$), 23.48 (s, CH(*C*H$_3$)$_2$); (*Anal.* Calc. for C$_{18}$H$_{32}$BKN$_4$ requires: C, 61.01; H, 9.10; N, 15.81. Found: C, 61.02; H, 8.97; N, 15.53%).

*4.3. Preparation of KTp^{iPr2}(HPz^{iPr2})$_3$ (**2**)*

A 50-mL round-bottomed flask was charged with KBH$_4$ (0.112 g, 2.080 mmol), *i*Pr$_2$pzH (2.000 g, 13.137 mmol), and a stir bar. The flask was then heated at 180 °C in an oil bath for 18 h, at which point gas evolution had ceased and the melt was a clear viscous liquid. The reaction mixture was cooled to room temperature, the resultant solid was dissolved in hexane (20 mL), and the solution was filtered through a 2-cm pad of Celite on a medium glass frit. The clear filtrate was set aside in an Erlenmeyer flask and slow evaporation at room temperature afforded colorless crystals of **2** (1.068 g, 53%): mp 147–149 °C; IR (Nujol, cm^{-1}) ν_{N-H} = 3261, 3358, ν_{B-H} = 2469, ν_{C-N} = 1565, 1529; ^{1}H NMR (CD$_2$Cl$_2$, 23 °C, δ) 9.98 (b, 3H, N*H*), 5.84 (s, 3H, C*H*), 5.79 (s, 3H, 4-C*H*), 4.90 (broad s, 1H, B*H*), 3.19 (septet, *J* = 6.9 Hz, 3H, C*H*(CH$_3$)$_2$), 2.87 (septet, *J* = 6.9 Hz, 6H, C*H*(CH$_3$)$_2$), 2.60 (septet, *J* = 6.8 Hz, 3H, C*H*(CH$_3$)$_2$), 1.21 (d, *J* = 6.4 Hz, 36H, CH(C*H*$_3$)$_2$), 1.03 (d, *J* = 6.4 Hz, 18H, CH(C*H*$_3$)$_2$), 0.99 (d, *J* = 7.2 Hz, 18H, CH(C*H*$_3$)$_2$); ^{13}C{^{1}H} NMR (toluene-*d*$_8$, 23 °C, ppm) 159.33 (s, *C*$_q$), 155.66 (s, *C*$_q$), 154.40 (broad s, 2*C*$_q$), 97.87 (s, 4-*C*H), 97.02 (s, 4-*C*H), 27.93 (s, *C*H(CH$_3$)$_2$), 27.30 (broad s, *C*H(CH$_3$)$_2$), 26.71 (s, *C*H(CH$_3$)$_2$), 23.67 (s, CH(*C*H$_3$)$_2$), 23.43 (s, CH(*C*H$_3$)$_2$), 23.02 (s, CH(*C*H$_3$)$_2$); (*Anal.* Calc. for C$_{54}$H$_{94}$B$_2$KN$_{12}$ requires: C, 67.46; H, 9.78; N, 17.49. Found: C, 67.64; H, 9.81; N, 17.76%).

4.4. Preparation of $CaBp_2(THF)_2$ (**3**)

A 100-mL Schlenk flask was charged with CaI_2 (0.200 g, 0.680 mmol), KBp (0.253 g, 1.360 mmol), and a stir bar. Tetrahydrofuran (30 mL) was added, resulting in the immediate formation of a white precipitate of KI. The reaction mixture was stirred for 18 h, at which point the volatile components were removed under reduced pressure to afford a white residue. Hexane (30 mL) was added to extract the product. The resulting solution was filtered through a 3-cm pad of Celite on a medium glass frit to yield a clear filtrate, which was placed in a −23 °C freezer for 24 h. Decanting of the solvent with a fine cannula, followed by vacuum drying at ambient temperature for 1 h, afforded colorless crystals of **3** (0.804 g, 64%): mp 115–116 °C; IR (Nujol, cm^{-1}) ν_{B-H} = 2263–2415, ν_{C-N} = 1500; ^1H NMR (CD_2Cl_2, 23 °C, δ) 7.59 (d, J = 1.8 Hz, 4H, C*H*), 7.41 (d, J = 1.8 Hz, 4H, C*H*), 6.13 (t, J = 1.8 Hz, 4H, C*H*), 3.71 (b, 4H, BH_2), 3.69 (m, 8H, CH_2CH_2O), 1.80 (m, 8H, CH_2CH_2O); $^{13}C\{^1H\}$ NMR (CD_2Cl_2, 23 °C, ppm) 139.82 (s, *C*H), 135.54 (s, *C*H), 104.29 (s, 4-*C*H), 69.03 (s, CH_2CH_2O), 25.69 (s, CH_2CH_2O); (*Anal.* Calc. for $C_{20}H_{32}B_2CaN_8O_2$ requires: C, 50.23; H, 6.74; N, 23.43. Found: C, 50.58; H, 6.69; N, 23.67%).

4.5. Preparation of $SrBp_2(THF)_2$ (**4**)

In a fashion similar to the preparation of **3**, treatment of SrI_2 (0.207 g, 0.606 mmol) with KBp (0.218 g, 1.172 mmol) afforded **4** as a white powder (0.250 g, 81%). The analytical sample and single crystals for the X-ray crystallographic analysis were obtained by crystallization from hexane at −23 °C: mp 118–121 °C; IR (Nujol, cm^{-1}) ν_{B-H} = 2264–2416, ν_{C-N} = 1502; ^1H NMR (CD_2Cl_2, 23 °C, δ) 7.57 (d, J = 2.4 Hz, 4H, C*H*), 7.46 (d, J = 1.8 Hz, 4H, C*H*), 6.14 (t, J = 1.8 Hz, 4H, 4-C*H*), 3.69 (m, 8H, CH_2CH_2O), 3.61 (broad s, 2H, BH_2), 1.78 (m, 8H, CH_2CH_2O); $^{13}C\{^1H\}$ NMR (CD_2Cl_2, 23 °C, ppm) 139.62 (s, *C*H), 135.44 (s, *C*H), 104.30 (s, 4-*C*H), 68.83 (s, CH_2CH_2O), 25.66 (s, CH_2CH_2O); (*Anal.* Calc. for $C_{20}H_{32}B_2N_8O_2Sr$ requires: C, 45.68; H, 6.13; N, 21.32. Found: C, 45.84; H, 6.09; N, 21.49%).

4.6. Preparation of $BaBp_2(THF)_4$ (**5**)

A 100-mL Schlenk flask was charged with BaI_2 (0.257 g, 0.657 mmol), KBp (0.245 g, 1.317 mmol), and a stir bar. Tetrahydrofuran (30 mL) was added, resulting in the immediate formation of a white precipitate of KI. The reaction mixture was stirred for 18 h, then the resulting mixture was filtered through a 3-cm pad of Celite on a medium glass frit to yield a clear filtrate. The filtrate was reduced in volume to about 10 mL, and the solution was place in a −23 °C freezer for 24 h. Decanting of the solvent with a fine cannula, followed by vacuum drying at ambient temperature for 1 h, afforded colorless crystals of **5** (0.150 g, 32%): mp 280–282 °C; IR (Nujol, cm^{-1}) ν_{B-H} = 2253–2448, ν_{C-N} = 1492; ^1H NMR (acetone-d_6, 23 °C, δ) 7.44 (d, J = 1.6 Hz, 8H, C*H*), 7.28 (d, J = 1.6 Hz, 8H, C*H*), 5.95 (t, J = 2.0 Hz, 4H, 4-C*H*), 4.07 (broad s, J = 4H, BH_2), 3.61 (m, 16H, CH_2CH_2O), 1.78 (m, 16H, CH_2CH_2O); $^{13}C\{^1H\}$ NMR (acetone-d_6, 23 °C, ppm) 139.24 (s, *C*H), 134.82 (s, *C*H), 103.36 (s, 4-*C*H), 68.03 (s, CH_2CH_2–O), 26.12 (s, CH_2CH_2–O); (0.5 equivalents of tetrahydrofuran was lost due to its lability at room temperature. *Anal.* Calc. for $C_{26}H_{44}B_2BaN_8O_{3.5}$ requires: C, 45.65; H, 6.49; N, 16.40. Found: C, 45.73; H, 6.39; N, 16.58%).

4.7. Preparation of $CaBp_2^{iPr2}(THF)_2$ (**6**)

In a fashion similar to the preparation of **4**, treatment of CaI_2 (0.205 g, 0.698 mmol) with KBp^{iPr2} (0.483 g, 1.362 mmol) afforded **6** as a white solid (0.352 g, 63%). The analytical sample and single crystals for the X-ray crystallographic analysis were obtained by crystallization from hexane at −23 °C: mp 112–113 °C; IR (Nujol, cm^{-1}) ν_{B-H} = 2285–2432, ν_{C-N} = 1527; ^1H NMR (CD_2Cl_2, 23 °C, δ), 5.76 (s, 4H, 4-C*H*), 3.63 (m, 8H, CH_2CH_2O), 3.38 (septet, J = 6.8 Hz, 8H, $CH(CH_3)_2$), 2.42 (septet, J = 6.8 Hz, 8H, $CH(CH_3)_2$), 1.79 (m, 8H, CH_2CH_2O), 1.18 (d, J = 6.6 Hz, 24H, $CH(CH_3)_2$), 0.94 (d, J = 7.5 Hz, 24H, $CH(CH_3)_2$); $^{13}C\{^1H\}$ NMR (CD_2Cl_2, 23 °C, ppm) 159.76 (s, C_q), 155.99 (s, C_q), 96.68 (s, 4-*C*H), 68.62 (s, CH_2CH_2O), 27.62 (s, $CH(CH_3)_2$), 26.42 (s, $CH(CH_3)_2$), 25.79 (s, CH_2CH_2O), 23.54 (s, 2 overlapping $CH(CH_3)_2$); (*Anal.* Calc. for $C_{44}H_{80}B_2CaN_8O_2$ requires: C, 64.85; H, 9.90; N, 13.75. Found: C, 64.46; H, 9.93; N, 13.96%).

4.8. Preparation of $SrBp_2^{iPr2}(THF)_2$ (**7**)

In a fashion similar to the preparation of **4**, treatment of SrI_2 (0.201 g, 0.589 mmol) with KBp^{iPr2} (0.415 g, 1.17 mmol) afforded **7** as a white solid (0.310 g, 61%). The analytical sample and single crystals for the X-ray crystallographic analysis were obtained by crystallization from hexane at −23 °C: mp 167–168 °C; IR (Nujol, cm^{-1}) ν_{B-H} = 2279–2429, ν_{C-N} = 1532; ^1H NMR (CD_2Cl_2, 23 °C, δ), 5.76 (s, 4H, 4-C*H*), 3.57 (m, 8H, CH_2CH_2O), 3.38 (septet, J = 6.9 Hz, 8H, $CH(CH_3)_2$), 3.38 (septet, J = 7.0 Hz, 8H, $CH(CH_3)_2$), 1.78 (m, 8H, CH_2CH_2O), 1.16 (d, J = 6.4 Hz, 24H, $CH(CH_3)_2$), 1.03 (d, J = 7.2 Hz, 24H, $CH(CH_3)_2$); $^{13}C\{^1H\}$ NMR (CD_2Cl_2, 23 °C, ppm) 159.44 (s, C_q), 156.02 (s, C_q), 96.33 (s, 4-*C*H), 68.51 (s, CH_2CH_2O), 28.15 (s, $CH(CH_3)_2$), 26.40 (s, $CH(CH_3)_2$), 25.75 (s, CH_2CH_2O), 23.75 (s, $CH(CH_3)_2$), 23.57 (s, $CH(CH_3)_2$); (*Anal.* Calc. for $C_{44}H_{80}B_2N_8O_2Sr$ requires: C, 61.28; H, 9.35; N, 12.99. Found: C, 61.30; H, 9.36; N, 12.95%).

4.9. Preparation of $BaBp_2^{iPr2}(THF)_2$ (**8**)

In a fashion similar to the preparation of **4**, treatment of BaI_2 (0.204 g, 0.522 mmol) with KBp^{iPr2} (0.363 g, 1.02 mmol) afforded **8** as a white solid (0.205 g, 48%). The analytical sample and single crystals for the X-ray crystallographic analysis were obtained by crystallization from hexane at −23 °C: mp 165–167 °C; IR (Nujol, cm^{-1}) ν_{B-H} = 2274–2426, ν_{C-N} = 1530; ^1H NMR (CD_2Cl_2, 23 °C, δ), 5.76 (s, 4H, 4-C*H*), 3.61 (m, 8H, CH_2CH_2O), 3.36 (septet, J = 6.6 Hz, 8H, $CH(CH_3)_2$), 2.66 (septet, J = 6.6 Hz, 8H, $CH(CH_3)_2$), 1.79 (m, 8H, CH_2CH_2O), 1.15 (d, J = 6.6 Hz, 24H, $CH(CH_3)_2$), 1.03 (d, J = 6.6 Hz, 24H, $CH(CH_3)_2$); $^{13}C\{^1H\}$ NMR (CD_2Cl_2, 23 °C, ppm) 159.28 (s, C_q), 156.12 (s, C_q), 96.48 (s, 4-*C*H), 68.32 (s, CH_2CH_2O), 28.14 (s, $CH(CH_3)_2$), 26.31 (s, $CH(CH_3)_2$), 25.78 (s, CH_2CH_2O), 23.83 (s, $CH(CH_3)_2$), 23.58 (s, $CH(CH_3)_2$); (*Anal.* Calc. for $C_{44}H_{80}B_2BaN_8O_2$ requires: C, 57.94; H, 8.84; N, 12.29. Found: C, 58.09; H, 8.61; N, 12.40%).

4.10. X-ray crystallographic structure determinations of **2–8**

Diffraction data were measured on a Bruker X8 APEX-II kappa geometry diffractometer with Mo radiation and a graphite monochromator. Frames were collected at 100 K with the detector at 40 mm and 0.3° between each frame, and were recorded for 10 s unless otherwise noted. APEX-II [26] and SHELX [27] software were used in the collection and refinement of the models. Crystals of **2** appeared as colorless thin fragments. About 97116 reflections were measured, yielding 17717 unique data (R_{int} = 0.121). Hydrogen atoms were placed in observed or calculated positions. Three sets of pendant isopropyl groups were described with positional disorder at C35, C36, C41, C42, and C54 and were refined using partial occupancy sites and held isotropic. Complex **3** crystallized as colorless rods. 48358 *hkl* data points were harvested, which averaged to 6392 data (R_{int} = 0.079). Hydrogen atoms were calculated or observed. The C–C bonds in the two disordered tetrahydrofuran ligands were held fixed at 1.54 Å and partial occupancies were assigned for C14, C15, C18, C19, and C20, which were kept isotropic during refinement. Crystals of **4** were obtained as colorless plates. 68843 reflections were counted, which averaged to 12155 independent data (R_{int} = 0.22). Hydrogen atoms were placed at calculated or observed positions. Statistically, this is a poor structure due to crystal quality, but certainly the overall connectivity of the complex is correct. Crystals of **5** were colorless fragments. 89094 total data were measured, averaging to 9799 unique data (R_{int} = 0.043). Hydrogen atoms were placed in observed or calculated positions. One of the tetrahydrofuran ligands was disordered in a 55/45 ratio at one carbon (C22). Complex **6** crystallized as colorless plates and yielded 72788 total data, of which 6198 were independent (R_{int} = 0.064). Hydrogen atom positions were either calculated or observed. The central Ca ion occupies a 2-fold rotation axis. Complex **7** produced crystalline colorless triangular plates. 56905 data were recorded to merge into 6299 data (R_{int} = 0.134). Hydrogen atoms were placed in calculated or observed positions. The crystal diffracted poorly, which required a 48 h collection time (30 s frames). There are typical large thermal parameters for parts of the isopropyl groups and the tetrahydrofuran ligands. The Sr ion occupies a crystallographic 2-fold rotation axis. Complex **8** is isostructural with **6** (*vide supra*). Crystals were colorless flat rods. 88165 data were integrated to net 9664 independent data. Hydrogen atoms were placed in calculated and observed positions. There was significant disorder and partial occupancies were assigned for atoms C4, C5, C6, C13, C14, C15, C19, C22, and O1. These atoms were held isotropic during refinement. The Ba ion occupies a crystallographic 2-fold rotation axis. Lowering the space group symmetry did not resolve the disorder.

Acknowledgement

We thank the Army Research Office (grant no. W911NF-07-01-0489) for generous support of this research.

Appendix A. Supplementary data

CCDC 783233, 783234, 783235, 783236, 783237, 783238, and 783239 contains the supplementary crystallographic data for **2**–**8**. These data can be obtained free of charge via http://www.ccdc.cam.ac.uk/conts/retrieving.html, or from the Cambridge Crystallographic Data Centre, 12 Union Road, Cambridge CB2 1EZ, UK; fax: (+44) 1223-336-033; or e-mail: deposit@ccdc.cam.ac.uk.

References

[1] M.J. Saly, M.J. Heeg, C.H. Winter, Inorg. Chem. 48 (2009) 5303.

[2] (a) M.J. Saly, F. Munnik, R.J. Baird, C.H. Winter, Chem. Mater. 21 (2009) 3742;
(b) M.J. Saly, F. Munnik, C.H. Winter, J. Mater. Chem. 20 (2010) 9995.

[3] (a) M. Leskelä, M. Ritala, Angew. Chem., Int. Ed. 42 (2003) 5548;
(b) L. Niinistö, J. Päiväsaari, J. Niinistö, M. Putkonen, M. Nieminen, Phys. Stat. Sol. A 201 (2004) 1443;
(c) M. Putkonen, L. Niinistö, Top. Organomet. Chem. 9 (2005) 125;
(d) R.L. Puurunen, J. Appl. Phys. 97 (2005) 121301;
(e) S.M. George, Chem. Rev. 110 (2010) 111.

[4] T.R. Belderraín, L. Contreras, M. Paneque, E. Carmona, A. Monge, C. Ruiz, Polyhedron 15 (1996) 3453.

[5] (a) H. Kokusen, Y. Sohrin, S. Kihara, M. Matsui, Anal. Sci. 7 (1991) 7;
(b) N. Yasuda, H. Kokusen, Y. Sohrin, S. Kihara, M. Matsui, Bull. Chem. Soc. Jpn. 65 (1992) 781;
(c) Y. Sohrin, H. Kokusen, S. Kihara, M. Matsui, Y. Kushi, M. Shiro, J. Am. Chem. Soc. 115 (1993) 4128.

[6] D.J. Loroño-Gonzalez, Acta Crystallogr., Sect. C: Cryst. Struct. Commun. 64 (2008) m229.

[7] M.J. Saly, C.H. Winter, Organometallics 29 (2010) 5472.

[8] S. Trofimenko, J. Am. Chem. Soc. 89 (1967) 3170.

[9] L. Maria, Â. Domingos, I. Santos, Inorg. Chem. Commun. 6 (2003) 58.

[10] N. Kitajima, K. Fujisawa, C. Fujimoto, Y. Moro-oka, S. Hashimoto, T. Kitagawa, K. Toriumi, K. Tatsumi, A. Nakamura, J. Am. Chem. Soc. 114 (1992) 1277.

[11] (a) C.M. Dowling, D. Leslie, M.H. Chisholm, G. Parkin, Main Group Chem. 1 (1995) 29;
(b) C. Dowling, P. Ghosh, G. Parkin, Polyhedron 16 (1997) 3469.

[12] K. Weis, H. Vahrenkamp, Inorg. Chem. 36 (1997) 5589.

[13] (a) M.H. Chisholm, J.C. Gallucci, G. Yaman, Chem. Commun. (2006) 1872;
(b) M.H. Chisholm, J.C. Gallucci, G. Yaman, Inorg. Chem. 46 (2007) 8676.

[14] (a) A. Bondi, J. Phys. Chem. 68 (1964) 441;
(b) M. Mantina, A.C. Chamberlin, S. Valero, C.J. Cramer, D.G. Truhlar, J. Phys. Chem. A 113 (2009) 5806.

[15] D.L. Reger, Y. Ding, A.L. Rheingold, R.L. Ostrander, Inorg. Chem. 33 (1994) 4226.

[16] (a) S. Trofimenko, Chem. Rev. 93 (1993) 943;
(b) S. Trofimenko, Scorpionates – The Coordination Chemistry of Polypyrazolylborate Ligands, Imperial College Press, London, 1999.

[17] S.G. Dutremez, D.B. Leslie, W.E. Streib, M.H. Chisolm, K.G. Caulton, J. Organomet. Chem. 462 (1993) C1.

[18] S. Harder, J. Brettar, Angew. Chem., Int. Ed. 45 (2006) 3474.

[19] M.J. Harvey, T.P. Hanusa, M. Pink, Chem. Commun. (2000) 489.

[20] P. Capporto, F. Mani, C. Mealli, Inorg. Chem. 17 (1978) 1232.

[21] D.L. Reger, J.A. Lindeman, L. Lebioda, Inorg. Chem. 27 (1988) 1890.

[22] A. Carvalho, Â. Domingos, P. Gaspar, N. Marques, A. Pires De Matos, I. Santos, Polyhedron 11 (1992) 1481.

[23] L. Maria, Â. Domingos, I. Santos, Inorg. Chem. 42 (2003) 3323.

[24] H.V.R. Dias, J.D. Gordan, Inorg. Chem. 35 (1996) 318.

[25] (a) L.J. Guggenberger, C.T. Prewitt, P. Meakin, S. Trofimenko, J.P. Jesson, Inorg. Chem. 12 (1973) 508;
(b) D.L. Reger, T.D. Wright, M.D. Smith, A.L. Rheingold, B. Rhagitan, J. Chem. Crystallogr. 30 (2000) 665.

[26] APEX II Collection and Processing Programs are Distributed by the Manufacturer, Bruker AXS Inc., Madison WI, USA, 2009.

[27] G.M. Sheldrick, Acta Crystallogr., Sect. A: Found. Crystallogr. 64 (2008) 112.